Molecular Microbiology (2012) 84(2), 370–382 ■
doi:10.1111/j.1365-2958.2012.08028.x
First published online 20 March 2012

Multiple ABC transporters are involved in the acquisition of petrobactin in *Bacillus anthracis*

Shandee D. Dixon, Brian K. Janes, Alexandra Bourgis, Paul E. Carlson Jr and Philip C. Hanna*
Department of Microbiology and Immunology, University of Michigan Medical School, Ann Arbor, MI 48104, USA.

Summary

In *Bacillus anthracis* the siderophore petrobactin is vital for iron acquisition and virulence. The petrobactin-binding receptor FpuA is required for these processes. Here additional components of petrobactin reacquisition are described. To identify these proteins, mutants of candidate permease and ATPase genes were generated allowing for characterization of multiple petrobactin ATP-binding cassette (ABC)-import systems. Either of two distinct permeases, FpuB or FatCD, is required for iron acquisition and play redundant roles in petrobactin transport. A mutant strain lacking both permeases, Δ*fpuB*Δ*fatCD*, was incapable of using petrobactin as an iron source and exhibited attenuated virulence in a murine model of inhalational anthrax infection. ATPase mutants were generated in either of the permease mutant backgrounds to identify the ATPase(s) interacting with each individual permease channel. Mutants lacking the FpuB permease and FatE ATPase (Δ*fpuB*Δ*fatE*) and a mutant lacking the distinct ATPases FpuC and FpuD generated in the Δ*fatCD* background (Δ*fatCD*Δ*fpuC*Δ*fpuD*) displayed phenotypic characteristics of a mutant deficient in petrobactin import. A mutant lacking all three of the identified ATPases (Δ*fatE*Δ*fpuC*Δ*fpuD*) exhibited the same growth defect in iron-depleted conditions. Taken together, these results provide the first description of the permease and ATPase proteins required for the import of petrobactin in *B. anthracis*.

Accepted 27 February, 2012. *For correspondence. E-mail pchanna@umich.edu; Tel. (+1) 734 615 3706; Fax (+1) 734 764 3562.

Introduction

Bacillus anthracis, a Gram-positive, spore forming bacterium, is the causative agent of the disease anthrax, which affects a wide range of mammals, including humans (Hanna, 1998a,b; Dixon *et al*., 1999). Over the course of its life cycle, *B. anthracis* exists in two distinct morphotypes, the metabolically active vegetative cell and the dormant spore. Vegetative bacilli within the host acquire enough nutrients to replicate rapidly and to very high titres (Dixon *et al*., 1999). Upon death of the host, the bacillus enters an environment lacking the nutrients required to sustain growth and replication, and sporulates (Dutz and Kohout, 1971; Dutz and Kohout-Dutz, 1981; Guidi-Rontani *et al*., 1999). The spores are the infectious particles of anthrax and are highly resistant to heat, cold, radiation, desiccation and disinfectants and persist in the environment in a dormant state until taken up by another host (Nicholson *et al*., 2000; Doganay and Welsby, 2006; Almeida *et al*., 2008).

Bacillus anthracis is capable of causing three forms of human disease, dependent on the route of spore entry into the host. While cutaneous and gastrointestinal anthrax are medical concerns, the most severe form of the disease is inhalational anthrax (Dixon *et al*., 1999; Inglesby *et al*., 1999; 2002; Doganay and Welsby, 2006). Mortality rates from this form of anthrax infection approach 45–50% (Spencer, 2003; Sweeney *et al*., 2011). Following inhalation, spores are taken up by alveolar phagocytes and transported to the lymph nodes, where the spores germinate and outgrowth to vegetative cells occurs (Dutz and Kohout, 1971; Dutz and Kohout-Dutz, 1981; Guidi-Rontani *et al*., 1999; Dixon *et al*., 2000). Eventually the replicating bacilli lyse the phagocytes and escape into the bloodstream, where they can reach titres of up to 10^8 bacilli per millilitre of blood (Dixon *et al*., 1999). As the bacteria multiply, they express virulence factors, most notably toxin, which ultimately leads to septic shock and death of the host within a few days (Dixon *et al*., 1999). Following host death, bacteria will sporulate once again and remain dormant until a suitable environment is encountered.

The robust growth rate of *B. anthracis* necessitates the need for highly efficient mechanisms for nutrient acquisition within the host (Ratledge and Dover, 2000; Faraldo-Gomez and Sansom, 2003; Wandersman and Delepelaire,

2004). One vital nutrient required for all bacteria is iron (Ratledge and Dover, 2000). Ferric iron (Fe^{3+}) is found in highly insoluble forms and is toxic to host cells through the formation of damaging oxygen radicals (Ratledge and Dover, 2000; Ratledge, 2004; Miethke and Marahiel, 2007; Davidson *et al*., 2008). Consequently, free iron concentrations in the host are low. The majority of iron in the mammalian host is bound to proteins such as haemoglobin, transferrin and ferritin (Ratledge and Dover, 2000; Glanfield *et al*., 2007). Since low concentrations of free iron can constitute a barrier against bacterial growth, the ability to acquire iron from the host is often a major determinant of microbial survival and virulence (Braun and Braun, 2002). To this end, pathogenic microbes, including *B. anthracis*, have evolved a variety of mechanisms to sequester iron from host proteins, including the production of siderophores (Ratledge and Dover, 2000; Faraldo-Gomez and Sansom, 2003; Glanfield *et al*., 2007).

Siderophores are high-affinity iron chelating molecules secreted in low iron environments to scavenge ferric iron from host proteins (Neilands, 1995; Zawadzka *et al*., 2009a). The production and secretion of siderophores is the primary mechanism of iron acquisition by *B. anthracis* (Ratledge and Dover, 2000). *B. anthracis* produces two distinct siderophore molecules, bacillibactin and petrobactin (Cendrowski *et al*., 2004b; Koppisch *et al*., 2005; Wilson *et al*., 2006; Lee *et al*., 2007; Pfleger *et al*., 2007; 2008b; Zawadzka *et al*., 2009a,b; Hotta *et al*., 2010) Petrobactin is the only siderophore essential for growth in macrophages and murine virulence (Garner *et al*., 2004; Cendrowski *et al*., 2004b; Koppisch *et al*., 2005; Abergel *et al*., 2006a; 2008). The siderophore bacillibactin, conversely, is thought to be dispensable during *B. anthracis* pathogenesis, as strains deficient in bacillibactin synthesis are fully virulent in a murine inhalational anthrax infection model (Cendrowski *et al*., 2004b). While both petrobactin and bacillibactin are catecholate siderophores, a possible explanation for their relative importance in pathogenesis may be found in their distinct chemical structures. Bacillibactin, commonly found in several *Bacillus* species (Koppisch *et al*., 2005), has a catecholate orientation (2,3-dihydroxybenzoate) widely observed in siderophores (Miethke and Marahiel, 2007), while petrobactin has a unique catecholate orientation (3,4-dihydroxybenzoate). This uncommon orientation allows this siderophore to evade recognition by the human immune protein siderocalin, thus petrobactin has been termed the 'stealth siderophore' of *B. anthracis* (Abergel *et al*., 2006a; Pfleger *et al*., 2008b; Zawadzka *et al*., 2009b).

The stages of petrobactin biosynthesis have been well studied in *B. anthracis* (Barbeau *et al*., 2002; Cendrowski *et al*., 2004a; Challis, 2005; Koppisch *et al*., 2005; 2008a,b; Wilson *et al*., 2006; 2009; Abergel *et al*., 2006b; 2008; Lee *et al*., 2007; 2011; Liu *et al*., 2007; Oves-Costales *et al*., 2007; 2009; 2008; Pfleger *et al*., 2007; 2008a; Fox *et al*., 2008; Kadi and Challis, 2009). However, only some of the details about iron-petrobactin import are known. We have previously shown that FpuA is the receptor protein required for normal growth under iron-depleted conditions and for murine virulence (Carlson *et al*., 2010). Furthermore, FpuA shows high sequence homology with the receptor components of ATP-binding cassette (ABC)-transport systems from other bacteria; therefore transport of iron-petrobactin most likely occurs through an ABC-transport system. Here we present the identification and characterization of the permease and ATPase components of the petrobactin ABC-import system.

Results

Identification of two individual permeases involved in petrobactin reacquisition

Seven iron-hydroxamate transporter permeases were identified as putative components of the *B. anthracis* petrobactin import system. Each of these proteins has significant sequence homology to the well-characterized ATP-dependent iron (III) hydroxamate permease (FhuB) from *Escherichia coli* (Koster, 2001; 2005), and all are induced by iron starvation (Carlson *et al*., 2009). Genetic organization of these putative permeases fall into two classes: those that are encoded by a single gene (GBAA4767, GBAA4596, GBAA4785 and GBAA5630), and those that are encoded by two consecutive genes (GBAA5328–5329, GBAA3865–3866 and GBAA0616–0617) (Fig. 1). Of these predicted permeases, the most obvious candidate for a role in petrobactin import was GBAA4767 (*fpuB*), as it is located directly downstream and likely co-transcribed with *fpuA*, which encodes the petrobactin receptor protein (Carlson *et al*., 2010). Another attractive candidate was the heterodimeric permease FatCD (GBAA5328–5329). An orthologue of this permease, YclNO, was previously shown to be required for petrobactin reacquisition in *B. subtilis* (Zawadzka *et al*., 2009b).

To test if any of these putative permease proteins were required for the import of petrobactin, individual mutants lacking each of the seven permeases were constructed and analysed. Each mutant was examined for the ability to grow in iron-depleted media (IDM). Mutants unable to synthesize or import petrobactin display a severe growth defect under these conditions (Cendrowski *et al*., 2004b; Carlson *et al*., 2010). Surprisingly, none of the single permease mutants, including Δ*fpuB* and Δ*fatCD*, exhibited a growth defect in IDM (Fig. 2A, solid squares and solid triangles, Fig. S1 and Table S1). It was therefore hypothesized that more than one of the putative permeases could facilitate the import of petrobactin. To test this, a mutant lacking the two most likely candidate permeases,

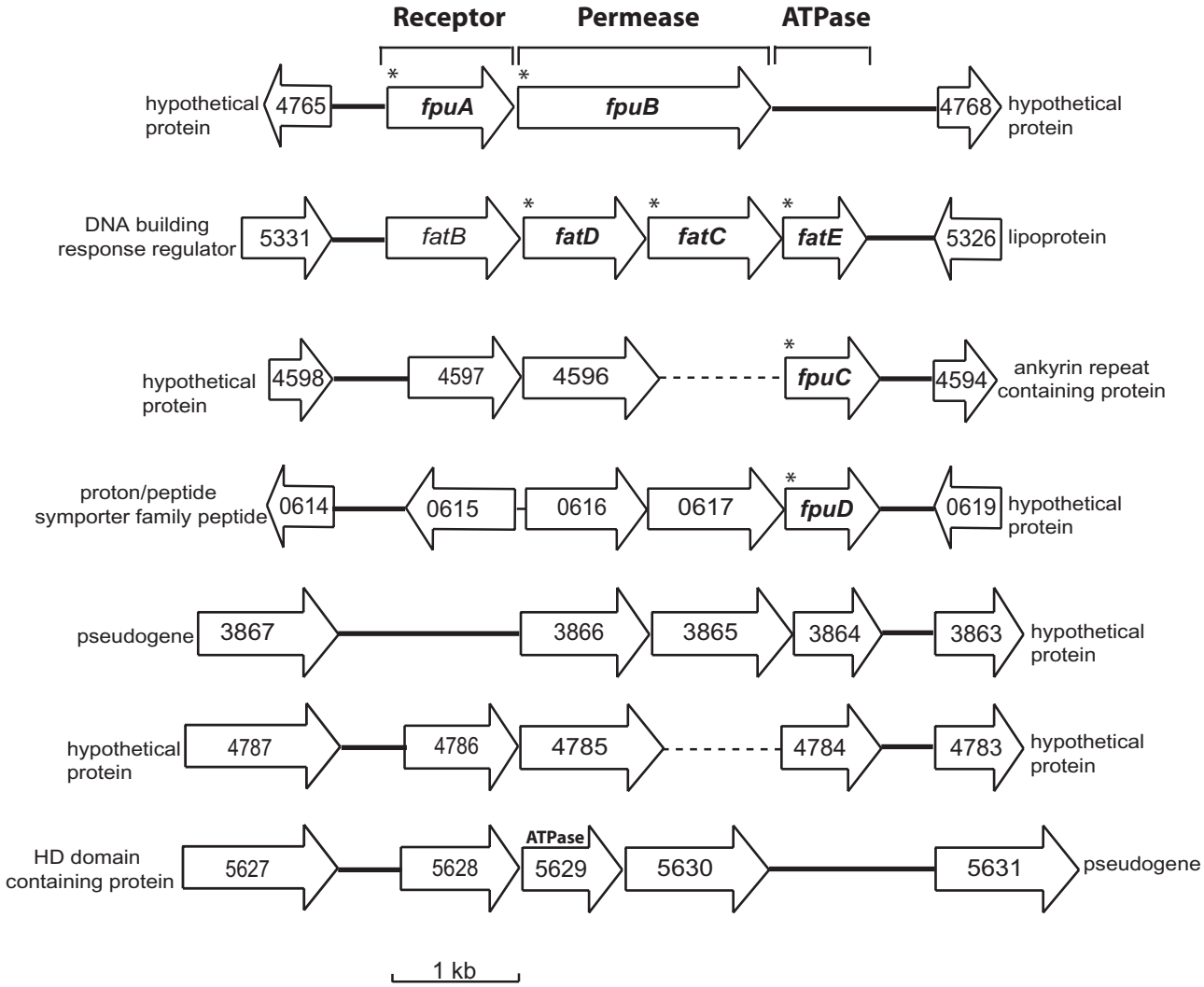

Fig. 1. Organization of genes investigated in this work. The genes encoding the iron-associated ABC-transporter components investigated in this work reside in seven separate clusters. Those found to be involved in the reacquisition of petrobactin belong to four of these clusters; individual genes directly involved in this process are marked with asterisks. Gene names for *fpuB* (GBAA4767; previously annotated as *fhuB*), *fpuC* (GBAA4595), *fpuD* (GBAA0618) and *fatE* (GBAA5327) have been updated to reflect their involvement in petrobactin transport. The three other gene clusters investigated here showed no involvement in this process. All clusters are aligned in the order receptor/permease/ATPase, with the exception of GBAA5629, which is labelled separately as this ATPase gene is positioned between the receptor and permease genes in its cluster. Dotted lines between consecutive genes were used for alignment purposes and do not indicate actual space between the genes. The annotated or predicted functions of all genes flanking each cluster are also shown. Intergenic region between the clusters and the flanking genes are not to scale.

FpuB and FatCD, was generated. The Δ*fpuB*Δ*fatCD* mutant exhibited a severe growth defect in IDM (Fig. 2A, open diamonds), similar to that of mutants deficient in both petrobactin transport (Δ*fpuA*) and petrobactin biosynthesis (Δ*asbABCDEF*) (Fig. 2A, open squares and open triangles respectively). These results suggest that these proteins play redundant roles in petrobactin transport. It is important to note that this growth defect was iron dependent, as all mutants tested exhibited wild-type growth levels in rich media (Fig. 2B, and data not shown).

To further demonstrate the role of these permeases in petrobactin import, it was necessary to eliminate the possibility that these mutants were unable to produce or secrete the siderophore. There are several phenotypes that can distinguish an import-deficient mutant (e.g. Δ*fpuA*), from a biosynthetic mutant (e.g. Δ*asbABCDEF*), including the inability to be chemically rescued with supplemental petrobactin, accumulation of extracellular catechol, and resistance to gallium toxicity (Carlson *et al.*, 2010). The first phenotype tested was the ability to be chemically rescued to wild-type growth levels in IDM by the addition of

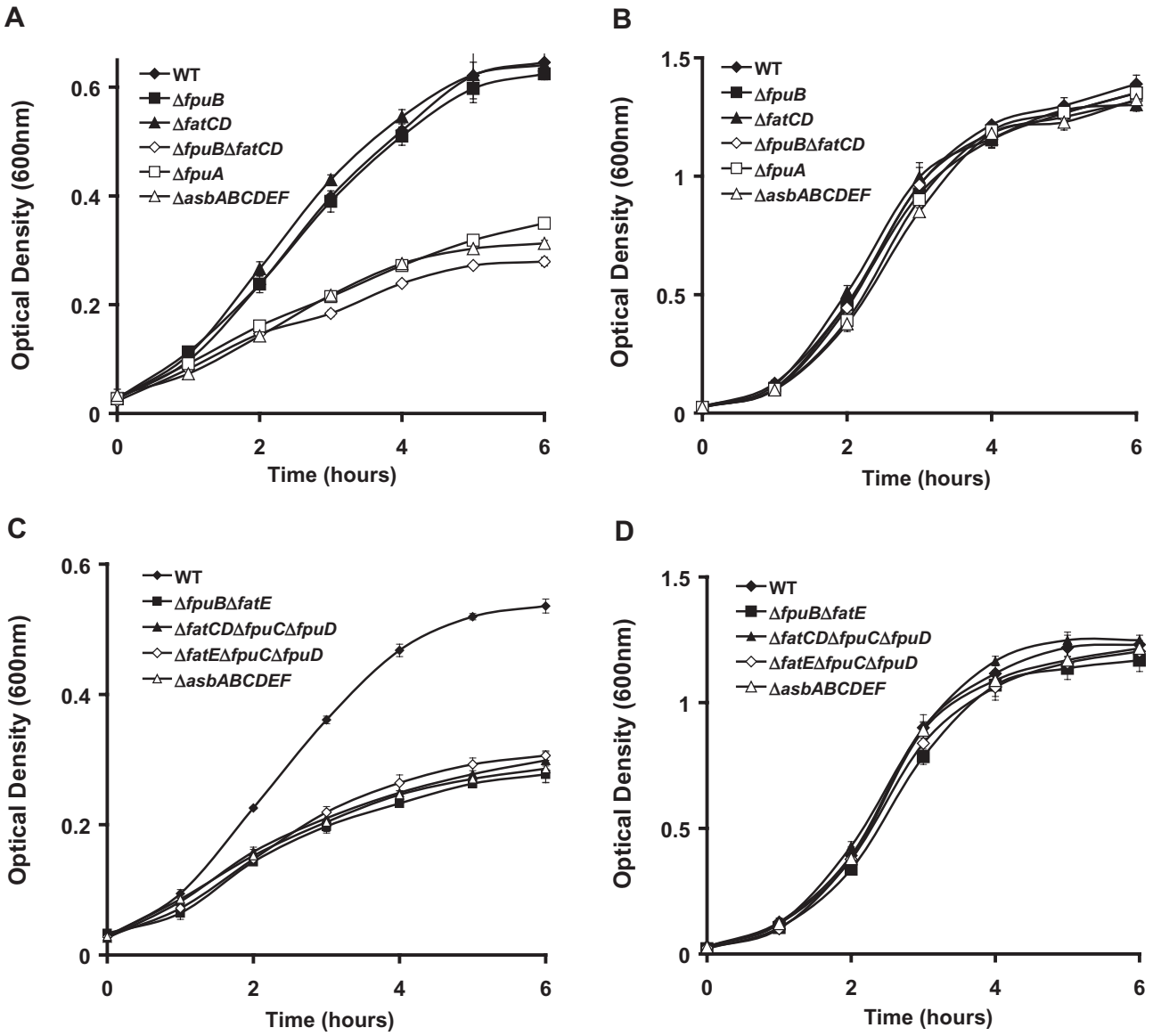

Fig. 2. Growth phenotypes of *B. anthracis* mutant strains. All cultures were inoculated with actively growing vegetative bacilli at an initial OD_{600} of 0.05. Growth was monitored hourly by measuring OD_{600}. Wild-type and Δ*asbABCDEF* strains were used in all experiments as controls.
A and B. Growth of permease deletion mutants. Wild-type (solid diamonds), Δ*fpuB* (solid squares), Δ*fatCD* (solid triangles), Δ*fpuB*Δ*fatCD* (open diamonds), Δ*fpuA* (open squares) and Δ*asbABCDEF* (open triangles) strains were grown in either IDM media (A) or BHI media (B).
C and D. Growth of ATPase deletion mutants. Wild-type (solid diamonds), Δ*fpuB*Δ*fatE* (solid squares), Δ*fatCD*Δ*fpuC*Δ*fpuD* (solid triangles), Δ*fatE*Δ*fpuC*Δ*fpuD* (open diamonds) and Δ*asbABCDEF* (open triangles) strains were grown in either IDM media (C) or BHI media (D).
Data are presented as mean ± standard deviation of triplicate measures from one experiment and represent at least three independent experiments.

exogenous petrobactin. This supplementation allows for recovery of growth of petrobactin biosynthetic mutants, while transport-deficient mutants are not complemented in this manner. Spores of wild-type, Δ*asbABCDEF*, Δ*fpuA* or Δ*fpuB*Δ*fatCD* strains were grown in IDM with or without supplemental petrobactin (2.5 μM). As expected, the growth of the petrobactin biosynthetic mutant was fully restored by this supplementation (Fig. 3A and B, solid triangles). However, this treatment did not restore growth of the double permease mutant (Δ*fpuB*Δ*fatCD*), indicating an inability to import petrobactin (Fig. 3A and B, open squares). This result was identical to that of the known petrobactin transport mutant (Δ*fpuA*) (Fig. 3A and B, solid circles) (Arnow, 1937; Carlson *et al.*, 2010).

A second phenotype of mutants unable to import petrobactin is significant accumulation of catechol in the culture

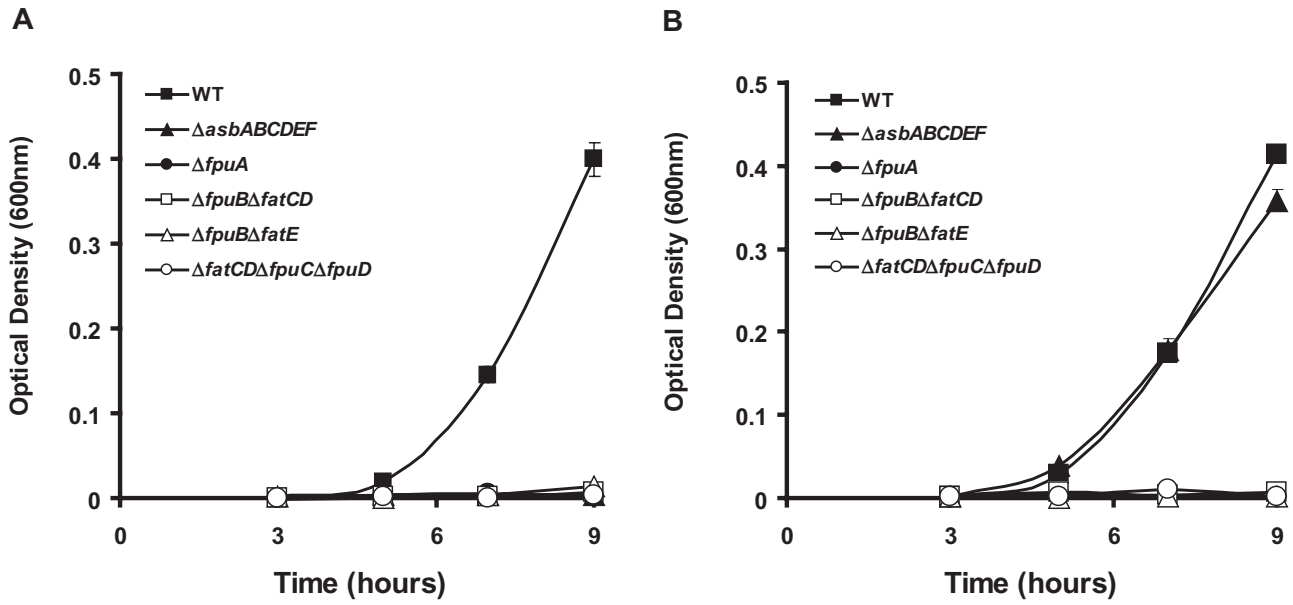

Fig. 3. Petrobactin supplementation does not restore growth of transport-deficient mutants in IDM. Cultures of either IDM (A) or in IDM supplemented with 2.5 μM purified petrobactin (B) were inoculated with 1×10^5 spores of wild-type (solid squares), Δ*asbABCDEF* (solid triangles), Δ*fpuA* (solid circles), Δ*fpuB*Δ*fatCD* (open squares), Δ*fpuB*Δ*fatE* (open triangles) or Δ*fatCD*Δ*fpuC*Δ*fpuD* (open circles). Growth was monitored by measuring OD_{600} over 9 h. Data are presented as mean ± standard deviation of triplicate measures from one experiment and represent at least three independent experiments.

supernatant, compared with that seen in wild-type strains (Carlson *et al*., 2010). The individual permease mutants, Δ*fpuB* and Δ*fatCD*, and the double mutant, Δ*fpuB*Δ*fatCD*, were assayed for extracellular catechol using the Arnow assay (Arnow, 1937). The petrobactin biosynthetic mutant was included as a control for non-petrobactin catechols. As reported previously (Carlson *et al*., 2010), culture supernantants from this strain exhibited minimal levels of catechol, indicating that the majority of what was observed is petrobactin (Fig. 4, Δ*asbABCDEF*). Catechol levels detected in the supernatants of all single permease mutants were nearly identical to those found in wild-type supernatants (Fig. 4). However, extracellular catechol levels in the culture supernatant of Δ*fpuB*Δ*fatCD* were significantly higher than those detected in wild type (Fig. 4). These results are similar to those obtained for Δ*fpuA*, which is unable to import petrobactin (Fig. 4 and Carlson *et al*., 2010).

The final phenotype tested was resistance to gallium toxicity. Gallium resistance has been used to show siderophore transport in several bacterial systems (Ecker and Emery, 1983; Olakanmi *et al*., 2000; Banin *et al*., 2008; Carlson *et al*., 2010). Gallium is able to bind to siderophores with high efficiency (Banin *et al*., 2008; Zawadzka *et al*., 2009b) and is toxic when imported into the bacterial cytoplasm (Banin *et al*., 2008). Previous studies have shown that the addition of 20 μM gallium sulphate to IDM culture media results in a petrobactin-dependent growth defect in wild-type *B. anthracis* (Carlson *et al*., 2010). To further test the ability of Δ*fpuB*-Δ*fatCD* to import petrobactin, growth of this strain was examined in the presence of gallium. Wild-type, Δ*asbABCDEF*, Δ*fpuA*, Δ*fpuB*, Δ*fatCD* and Δ*fpuB*Δ*fatCD* strains were incubated in the presence or absence of gallium sulphate and growth was measured by change in OD_{600} after 2 h. The addition of gallium sulphate to wild-type *B. anthracis* resulted in a significant growth inhibition when compared with cultures grown without gallium (Fig. 5). In contrast, strains unable to produce or import petrobactin are protected from this toxicity (Fig. 5, Δ*fpuA* and Δ*asbABCDEF*) (Cendrowski *et al*., 2004b; Carlson *et al*., 2010). As predicted by their ability to grow in IDM, both single permease mutants (Δ*fpuB* and Δ*fatCD*) were significantly inhibited by the presence of gallium (Fig. 5). Much like the petrobactin biosynthetic mutant, the double permease mutant, Δ*fpuB*Δ*fatCD*, was not significantly inhibited by the presence of gallium (Fig. 5).

The ΔfpuBΔfatCD *mutant is attenuated for virulence in a murine model of inhalational anthrax*

Known petrobactin biosynthetic (Δ*asbABCDEF*) and receptor (Δ*fpuA*) mutants exhibit significant attenuation in murine virulence (Cendrowski *et al*., 2004b; Carlson *et al*., 2010). Therefore, it was hypothesized that a strain lacking all permease components of the petrobactin import system would exhibit a similar attenuation. To test this hypothesis, a murine model of inhalational anthrax

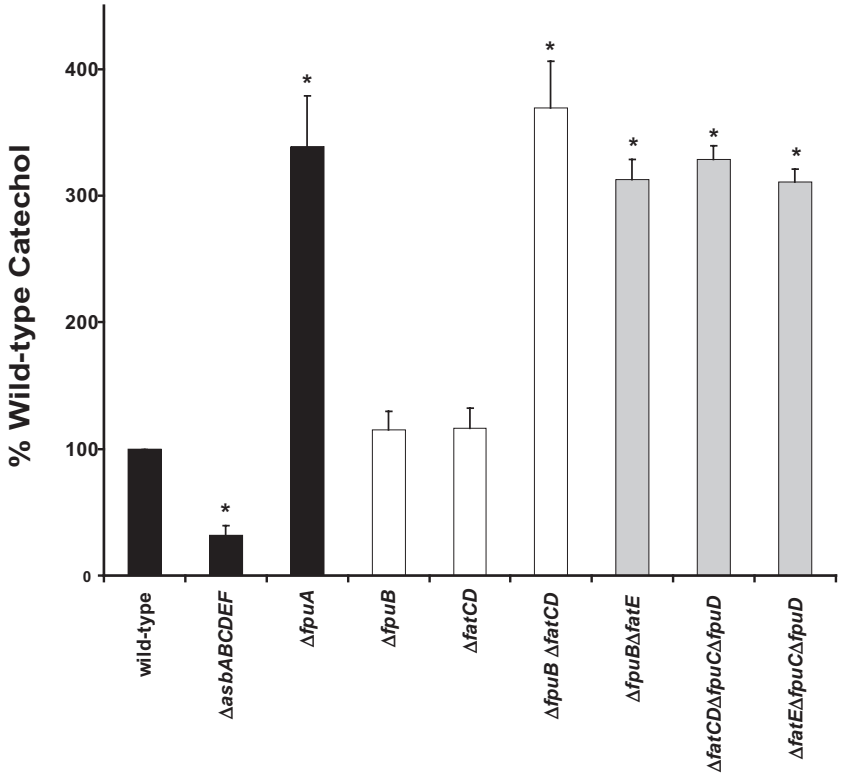

Fig. 4. Accumulation of extracellular catechols in petrobactin transport-deficient strains. Catechols were measured in filtered culture supernatants following 6 h growth of either control strains (black bars), permease mutants (white bars) or ATPase mutants (grey bars) using the Arnow assay. Data were normalized to the OD_{600} of cultures and are presented as per cent of wild-type catechol levels. Data are presented as mean ± standard deviation of triplicate measures from one experiment and represent three or more independent experiments. $^*P \leq 0.005$. The level of catechol observed from Δ*fpuB*Δ*fatCD* is not statistically significant ($P = 0.52$) from Δ*fpuA*.

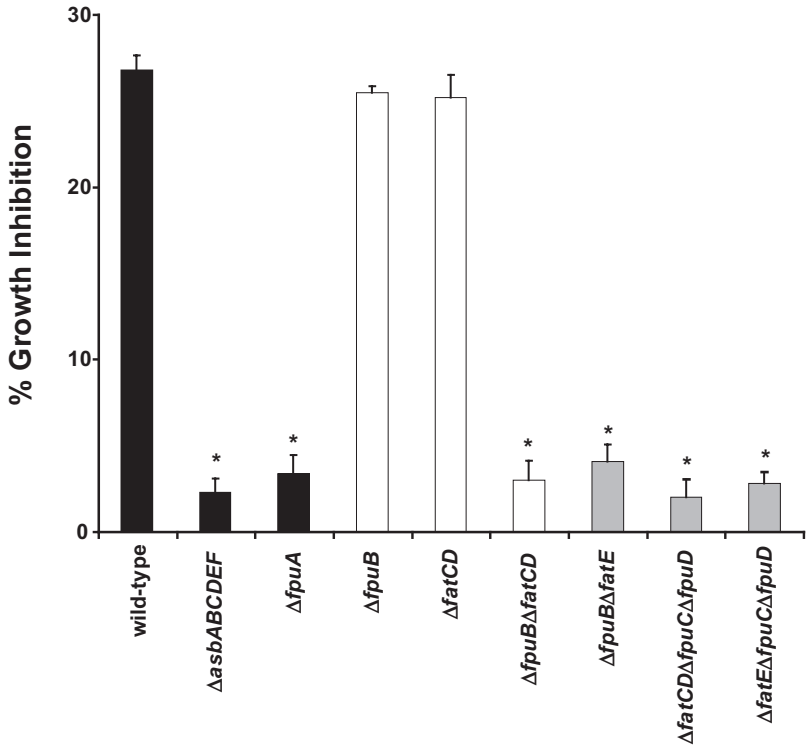

Fig. 5. Resistance of petrobactin transport-deficient strains to gallium toxicity. Control strains (black bars), permease mutants (white bars) or ATPase mutants (grey bars) were grown in IDM with or without 20 μM gallium sulphate and examined for change in OD_{600} after 2 h. Results are presented as per cent growth inhibition in the presence of 20 μM gallium sulphate. Data are presented as mean ± standard deviation of triplicate measures from one experiment and represent at least three independent experiments. $^*P \leq 0.0001$. Percent growth inhibition was calculated as {[(OD_{600} IDM + gallium)/(OD_{600} IDM)] × 100}.

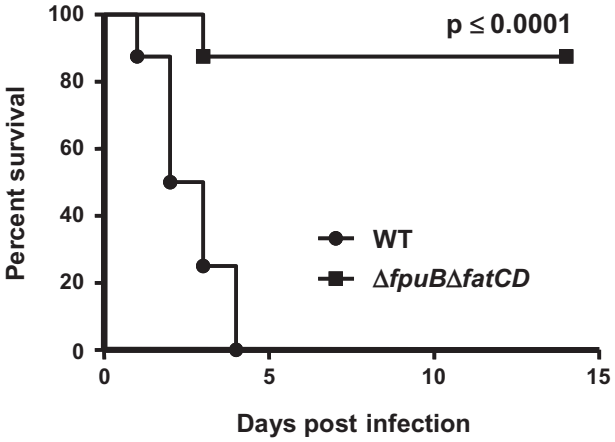

Fig. 6. Attenuation of double permease mutant in murine model of inhalational anthrax. DBA/2J mice were infected via intratracheal inoculation with either wild-type (solid circles, $n = 8$) or Δ*fpuB*Δ*fatCD* (solid squares, $n = 16$) mutant spores at a dose of 1×10^5 spores per mouse. Mice were monitored for 14 days after infection. The survival curve for the Δ*fpuB*Δ*fatCD* strain was significantly different from wild type by the log-rank test ($P \leq 0.0001$).

was used (Cendrowski *et al.*, 2004b). Mice were inoculated intratracheally with either wild-type ($n = 8$) or Δ*fpuB*-Δ*fatCD* ($n = 16$) spores at a dose of approximately 20 times the LD_{50} (1×10^5 spores per mouse). Mice were then monitored for 14 days post infection. As expected, all mice infected with wild-type spores succumbed to infection within 4 days (Fig. 6, circles) (Cendrowski *et al.*, 2004b). In sharp contrast, mice inoculated with the Δ*fpuB*-Δ*fatCD* strain exhibited a significant increase in survival ($P \leq 0.0001$), with the majority of mice (15 of 16) surviving the full 2-week experiment (Fig. 6, solid squares).

Identification of three ATPase components involved in petrobactin transport

A similar approach was taken to identify the ATPase components of the petrobactin transport system. Six ATPase proteins were identified as candidates for a role in petrobactin import. These putative ATPases are encoded by GBAA4595, GBAA0618, GBAA5629, GBAA4784, GBAA3864 and GBAA5327 (Fig. 1). To assess the putative role of these candidate proteins in petrobactin transport, six single-deletion mutants were generated, each lacking one of these genes. Similar to what was observed for the permeases, none of these single mutants exhibited a growth defect in IDM (Fig. S1 and Table S1). These findings, and the identification of two distinct petrobactin-specific permeases as described above, suggested the possibility that distinct ATPases could be functioning individually with each permease. Of the six putative ATPases, *fatE* is located directly downstream of *fatCD* and was, therefore, the most likely candidate to function with this permease. To determine whether FatE was functioning with the FatCD permease, it was necessary to prevent transport through the other permease, FpuB. Therefore, a mutant lacking the FatE ATPase was generated in the Δ*fpuB* background. This mutant, Δ*fpuB*Δ*fatE*, displayed all of the hallmark characteristics of a petrobactin import mutant including a growth defect in IDM (Fig. 2C, solid squares), an inability to be restored to wild-type growth levels by the addition of exogenous petrobactin (Fig. 3A and B, open triangles), increased extracellular catechol levels in culture supernatants (Fig. 4, grey bars), and resistance to gallium induced growth inhibition (Fig. 5, grey bars). These phenotypes combined implicate FatE in petrobactin import through interaction with the FatCD permease.

In order to identify the ATPase(s) functioning with the FpuB permease, an analogous approach was taken. Each of the remaining five putative ATPase genes was deleted individually in the Δ*fatCD* background. However, none of these mutants exhibited a growth defect in IDM (data not shown). This result suggested that multiple ATPases were functioning with this single permease. To test this, a double ATPase deletion mutant was generated in the Δ*fatCD* background targeting the two genes (GBAA4595 and GBAA0618) having the highest amino acid sequence identity to the FhuC ATPase from *E. coli* (45% and 42% identity respectively). This mutant, Δ*fatCD*-Δ*fpuC*Δ*fpuD*, displayed all of the phenotypic characteristics of a mutant deficient in petrobactin import. These included an inability to grow to wild-type levels in IDM (Fig. 2C, solid triangles), an inability to be restored to wild-type growth levels by the addition of exogenous petrobactin (Fig. 3A and B, open circles), increased extracellular catechol levels in culture supernatants (Fig. 4, grey bars), and protection from gallium induced growth inhibition (Fig. 5, grey bars). We therefore propose naming these genes *fpuC* (GBAA4595) and *fpuD* (GBAA0618). A mutant lacking only these two ATPases, but still encoding the FatCD permease (Δ*fpuC*Δ*fpuD*) did not have a growth defect in IDM (data not shown). Indeed, no mutant lacking two of these ATPases (*fatE*, *fpuC* or *fpuD*) showed any phenotype. All of these data combine to implicate the ATPases encoded by *fpuC* and *fpuD* in the import of petrobactin through interaction with the FpuB permease.

Finally, a mutant lacking all three ATPase components was constructed (Δ*fatE*Δ*fpuC*Δ*fpuD*). This strain retained wild-type copies of both of the identified petrobactin reacquisition permeases. The triple ATPase mutant exhibited the expected growth defect in IDM (Fig. 2C, open diamonds). As expected, the Δ*fatE*Δ*fpuC*Δ*fpuD* mutant also exhibited increased catachol levels (Fig. 4, grey bars), and no sensitivity to gallium (Fig. 5, grey bars). However, in addition to the growth defect observed in

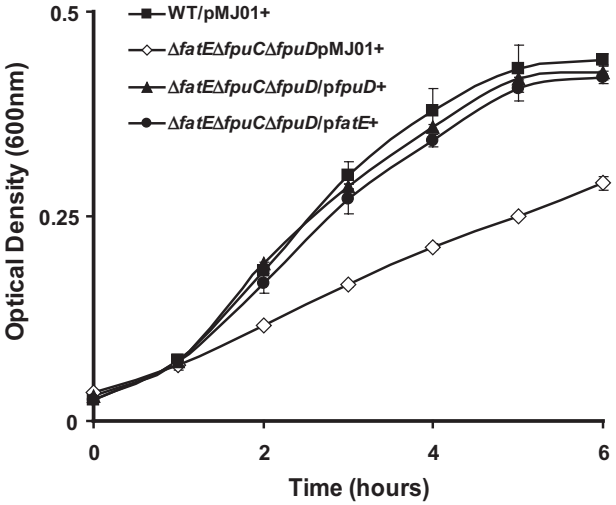

Fig. 7. Complementation of triple ATPase mutant. All cultures were inoculated with vegetative bacilli at an initial OD_{600} of 0.05 and growth was monitored hourly for 6 h by measuring increase in OD_{600}. Wild type/pMJ01+ and Δ*fatCD*Δ*fpuC*Δ*fpuD*/pMJ01+ strains were used as empty vector controls. Wild type/pMJ01+ (solid squares), Δ*fatE*Δ*fpuC*Δ*fpuD*/pMJ01+ (open diamonds), Δ*fatE*Δ*fpuC*Δ*fpuD*/p*fpuD*+ (solid triangles), Δ*fatE*Δ*fpuC*Δ*fpuD*/p*fatE*+ (solid circles) strains were grown in IDM media containing 10 μg ml^{-1} chloramphenicol. Data are presented as mean ± standard deviation of triplicate measures from one experiment and represent at least three independent experiments.

IDM, this mutant grew poorly in sporulation media, and failed to sporulate efficiently. Due to the inability to isolate spores, the petrobactin supplementation assay could not be performed. Although the mutant failed to grow well in sporulation media, it did not exhibit a general growth defect, as it grew as well as wild type in rich media (Fig. 2D, open diamonds) or in IDM supplemented with 20 μM ferrous sulphate (data not shown). The growth and sporulation defects observed for the *ΔfatEΔfpuCΔfpuD* mutant could be complemented *in trans*. Growth in IDM was restored to wild-type levels when either *fpuD* or *fatE* was expressed from a plasmid (Fig. 7, solid triangles and solid circles respectively). The ability to grow well in sporulation media and produce spores was restored in the complemented strains as well (data not shown). For unknown reasons, attempts to complement *fpuC* were unsuccessful.

Discussion

Bacillus anthracis encodes a number of genes involved in scavenging iron from a variety of sources, including those responsible for the biosynthesis of two siderophores (Lee *et al*., 2007; Carlson *et al*., 2009). However, both murine virulence and the ability to grow in iron-depleted medium *in vitro* are only dependent on the ability to produce and reacquire one of these molecules, petrobactin. Previous work established both the importance of petrobactin biosynthesis, and the requirement of the petrobactin receptor FpuA in its utilization (Cendrowski *et al*., 2004b; Garner *et al*., 2004; Lee *et al*., 2007; Carlson *et al*., 2009; 2010). The work presented here identifies two permeases and three ATPases that also function in petrobactin import. These proteins appear to function with the petrobactin receptor FpuA, presumably making at least three ABC-transporter complexes, each independently sufficient for the reacquisition of petrobactin (Fig. 8). Two of these transporter complexes involve association of the receptor, FpuA, with the FpuB permease. In turn, FpuB can function with either of two separate ATPases, FpuC or FpuD (Fig. 8, complexes A and B). The third transporter complex consists of FpuA associated with the FatCD permease and the FatE ATPase (Fig. 8, complex C).

While it is common for all of the components of a bacterial ABC transporter to be encoded within a single operon, instances exist where the genes encoding these components are located in separate positions on the genome. The genes that encode the components for petrobactin acquisition exhibit this partially unclustered genetic organization. The genes encoding FpuA and FpuB belong to a single operon lacking a gene encoding an ATPase (Fig. 1). Two distinct genes (*fpuC* and *fpuD*), found at separate locations on the chromosome, encode ATPase components that can individually energize import through FpuB (Fig. 8, complex A and B). These genes belong to otherwise uncharacterized iron-transport clusters containing both putative receptor and permease genes (Fig. 1) that play no apparent role in petrobactin reacquisition. For the FpuA/FatCDE transport complex (Fig. 8, complex C), the genes encoding the permease and ATPase components are contained within the same operon, *fatBCDE*. FatB, an apparent substrate-binding protein, is not required for petrobactin import, but may serve some other undefined role (Carlson *et al*., 2010).

Often the components of ABC transporters are unique to an individual transporter, although some promiscuity, similar to what is reported here for petrobactin import, has been observed. For example, the MsmK ATPase from *Streptococcus pneumoniae* associates with the transmembrane domains of multiple carbohydrate transporters, including those involved in the import of sialic acid (SatABC), raffinose (RafEGF) and maltotetraose (MalXCD) (Marion *et al*., 2011). Additionally, the FhuC ATPase from *Staphylococcus aureus* functions as the ATPase component of three distinct iron-siderophore transporters, HtsABC, SirABC and FhuCBG. These transporters are required for staphyloferrin A, staphyloferrin B and hydroxamate-mediated iron acquisition respectively (Beasley and Heinrichs, 2010). Similarly, the plasmid-encoded anguibactin uptake system of *Vibrio anguillarum* lacks an ATPase, and relies on a yet unidentified enzyme

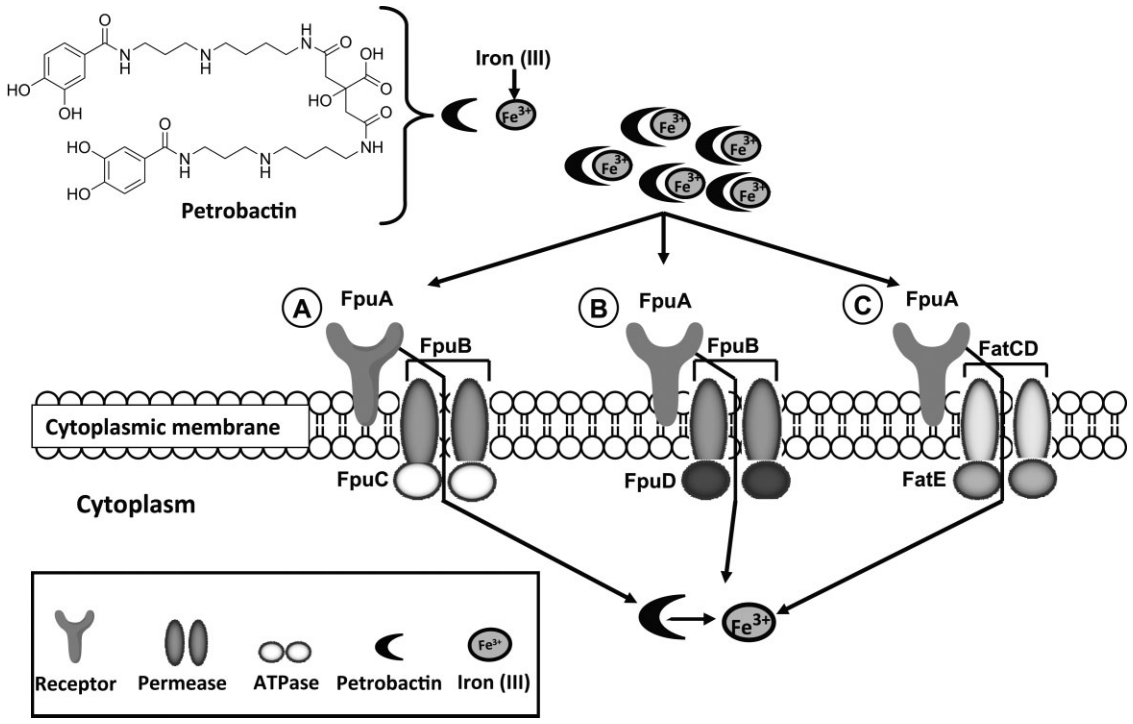

Fig. 8. Proposed model for *Bacillus anthracis* petrobactin ATP-binding cassette (ABC) import. Extracellular petrobactin (black crescents) binds to ferric iron ions (grey ovals) prior to reacquisition. The proteins required for the import of petrobactin include the substrate-binding receptor protein FpuA (required in all three complexes), two hydrophobic membrane-spanning domains, or permeases, FpuB (complex A and B) and FatCD (complex C), and three cytoplasmic ATPase domains, FatE, and proteins FpuC and FpuD that couple the energy of ATP hydrolysis to import petrobactin. It is presumed that the iron-siderophore complex is imported through the cytoplasmic membrane via one of these three canonical (substrate-binding protein dependent) ABC-transport protein complexes.

encoded on the chromosome (Koster *et al*., 1991; Lopez and Crosa, 2007). The work presented here reports an unusual inverse of these configurations in which a single substrate-binding protein, FpuA, presents petrobactin to two distinct permeases and furthermore, these two permease proteins display association with discrete ATPases.

Despite the compelling genetic analysis presented here suggesting three complexes following the canonical model for ABC transporters (Eitinger *et al*., 2011), we note that protein–protein interaction studies have not been performed. Additional characterizations, including the relative abundance of each transporter on the cell surface and preference of the receptor FpuA for the permeases FpuB or FatCD remain to be determined. Also, the question of when iron is removed from petrobactin, before or after import, remains. Considering the similarity in structure of petrobactin to other well-characterized siderophores including aerobactin (Koster and Braun, 1990a,b; Wooldridge *et al*., 1992) and bacillibactin (Miethke *et al*., 2006), it is likely that the intact ferric-petrobactin holocomplex is transported across the membrane. According to this model, reduction of the metal (Miethke and Marahiel, 2007) or degradation of the siderophore (Miethke *et al*., 2006; Garénaux *et al*., 2011) by currently unidentified enzymes would then allow for release of iron in the bacterial cytoplasm. However, the possibility exists that the release of iron from petrobactin occurs prior to internalization. This has been observed in *Salmonella typhimurium* and in *Mycobacterium tuberculosis* where the enzymatic reduction and release of iron from either ferrioxamine or mycobactin, respectively, occurs by extracellular iron reductases (Cowart, 2002; Ratledge, 2004).

We propose that the permeases FpuB and FatCD play redundant roles in petrobactin import, with either protein able to associate with their respective ATPases and the FpuA receptor in the formation of a canonical ABC-transport complex. Additional redundancy is observed by the association of FpuB with two ATPases, FpuC or FpuD (Fig. 8, complexes A and B), either of which is sufficient for petrobactin import. The genes that encode these two ATPases belong to gene clusters that contain both receptor and permease components and have high homology to other ABC transporters involved in ion transport (Fig. 1, GBAA4597 and GBAA0615 gene clusters). It seems likely, therefore, that these ATPases are functional components of transporters with roles other than petrobactin acquisition. A possible example of this multi-functionality is demonstrated by the growth defect of the triple mutant (Δ*fatE*Δ*fpuC*Δ*fpuD*) in sporulation media, a defect not

Table 1. *Bacillus anthracis* strains used in this study.

Strain/genotype	Relevant characteristics	Reference
Sterne 34F2	Wild type (pXO1$^+$, pXO2$^-$)	Sterne (1939)
34F2, Δ*asbABCDEF*	Petrobactin biosynthesis mutant	Lee *et al.* (2007)
34F2, Δ*fpuA*	Petrobactin receptor mutant	Carlson *et al.* (2010)
34F2, Δ*fpuB*		This work
34F2, Δ*fatCD*		This work
34F2, Δ*fpuB*Δ*fatCD*	Δ*fatCD* into Δ*fpuB*	This work
34F2, ΔGBAA0616–0617		This work
34F2, ΔGBAA3865–3866		This work
34F2, ΔGBAA4596		This work
34F2, Δ*fpuC*		This work
34F2, Δ*fpuD*		This work
34F2, ΔGBAA5629		This work
34F2, ΔGBAA4784		This work
34F2, ΔGBAA3864		This work
34F2, Δ*fatE*		This work
34F2, Δ*fpuB*Δ*fatE*	Δ*fatE* into Δ*fpuB*	This work
34F2, Δ*fatCD*Δ*fpuC*	Δ*fpuC* into Δ*fatCD*	This work
34F2, Δ*fatCD*Δ*fpuD*	Δ*fpuD* into Δ*fatCD*	This work
34F2, Δ*fatCD*Δ*fpuC*Δ*fpuD*	Δ*fpuD* into Δ*fatCD*Δ*fpuC*	This work
34F2, Δ*fpuC*Δ*fpuD*	Δ*fpuC* into Δ*fpuD*	This work
34F2, Δ*fatE*Δ*fpuC*	Δ*fatE* into Δ*fpuC*	This work
34F2, Δ*fatE*Δ*fpuD*	Δ*fatE* into Δ*fpuD*	This work
34F2, Δ*fatE*Δ*fpuC*Δ*fpuD*	Δ*fatE* into Δ*fpuC*Δ*fpuD*	This work

present in any other mutant, independent of their growth phenotypes in IDM. This inability to produce spores is most likely the result of the poor growth in the sporulation media, versus a defect in the sporulation machinery. However, the exact nature of this defect is unknown.

Petrobactin-facilitated iron uptake is a determinant of *B. anthracis* virulence. Through this, and previous work, we have completed the identification of components composing the import machinery facilitating this process. The petrobactin import system consists of redundant gene products that interact with specific partners in the formation of three canonical ABC-transport complexes (Fig. 8, complexes A, B and C). The description of siderophore uptake systems provides the identification of potential therapeutic targets for combating bacterial infections and creates a more accurate model of steps critical to the life cycle *B. anthracis* during pathogenesis. These findings also highlight the importance of host iron acquisition mechanisms during bacterial infection.

Experimental procedures

Bacterial growth and sporulation conditions

Bacterial strains used for this study are described in Table 1. All mutant strains were derived from the *B. anthracis* Sterne 34F$_2$ strain (pXO1$^+$, pXO2$^-$). Spores were generated as described previously (Passalacqua and Bergman, 2006), except that growth of the cultures was performed at 37°C and purified by passage through a 3.1 micron glass microfibre filter (National Scientific Company) to increase purity. Spore stocks were stored at room temperature in sterile water and titred using a haematocytometer to the desired concentration for use in mouse infection and petrobactin supplementation studies. All subsequent experiments were performed from these stocks. For experiments performed under low iron conditions, IDM was prepared as previously described (Cendrowski *et al.*, 2004b). For IDM growth experiments, overnight cultures grown in brain heart infusion broth (BHI) were back-diluted 1:50 in fresh medium and allowed to grow for 1 h at 37°C. Actively growing cells were collected by centrifugation at 1600 *g*, and the pellets were washed five times in IDM to remove residual iron. The washed cells were inoculated into IDM at a final optical density at 600 nm (OD_{600}) of 0.05. For complementation experiments, cultures were supplemented with 10 μg ml^{-1} chloramphenicol where indicated for plasmid maintenance. Cultures were grown at 37°C with aeration, and the OD_{600} was measured hourly for 6 h. For experiments performed with supplemental petrobactin, cultures were inoculated with 1×10^5 spores of the specified strains in 2 ml of IDM with or without the addition of 2.5 μM petrobactin (Carlson *et al.*, 2010), and were monitored for change in OD_{600} over 9 h. For gallium sensitivity assays, strains were inoculated into IDM, as described above, with or without the addition of 20 μM gallium sulphate. Results of the gallium sensitivity assay were normalized to culture OD_{600} and are presented as per cent growth inhibition and calculated as $\{[(OD_{600}\ \text{IDM} + \text{gallium})/(OD_{600}\ \text{IDM})] \times 100\}$ at 2 h (Carlson *et al.*, 2010).

Isolation of mutants and construction of complementation plasmids

Mutant strains isolated for this work were all constructed via allelic exchange. Each mutant allele was constructed via PCR using Phusion High Fidelity DNA polymerase

(New England Biolabs) according to the manufacturer's instructions. The PCR products were first cloned into the TOPO® cloning vector (Invitrogen), using manufacturer protocols, and the DNA sequence was verified (University of Michigan DNA sequencing core). The mutant allele was then cloned into the NotI site of the allelic exchange vector pBKJ258 (Janes and Stibitz, 2006) using standard methods. Each construct contained approximately 500 bp both upstream and downstream of the target gene with NotI restriction sites on each end for subsequent cloning. Each mutant allele retained the first 10 codons, followed by the DNA sequence GGGCCCTCCGGATCCCCCGGG, and then the last nine codons plus the predicted stop codon. A similar strategy was followed for each single gene deletion mutant. For mutations where two sequential genes were deleted, the initial 10 codons of the first gene were fused with the final nine codons of the second gene, in the same manner described above. Allelic exchange was performed as described previously (Janes and Stibitz, 2006). The presence of the mutant alleles was verified by PCR, and each resulting mutant was otherwise isogenic to the parental strain. Sequences of all oligonucleotides used in the creation and screening of these mutants are available upon request. Spore stocks for each mutant were generated and stored as described above.

PCR was used to amplify *fatE* and *fpuD* by standard methods. DNA fragments were cloned and each DNA sequence verified as described above for mutant allele construction. Primers were designed such that an XbaI site was inserted directly upstream of the initiation codon of the gene of interest, and a HindIII site directly downstream of the native stop codon. Each gene was cloned into the XbaI and HindIII sites of pGFP (Wilson *et al*., 2012), replacing the *gfpmut3a* allele with the gene of interest, expressed by the *p43* promoter present on the plasmid. The plasmid pMJ01, a version of pGFP lacking the *gfpmut3a* allele was used as a control (Wilson *et al*., 2012). Plasmids were passaged through SCS110 (*dam dcm*) and then transferred into the appropriate *B. anthracis* strain via electroporation (Passalacqua and Bergman, 2006).

Measurement of catechol accumulation

The levels of extracellular catechol were measured using the Arnow assay (Arnow, 1937; Carlson *et al*., 2010). Strains were grown as described above for 6 h and supernatants were collected and filtered using a 0.22 μm syringe filter. Culture supernatants were then mixed with equal volumes of 0.5 M HCl, followed by the sequential addition of equal volumes of nitrate-molybdate reagent (10% sodium nitrate and 10% sodium molybdate), 1 N NaOH and distilled H_2O in 96-well plates. Sample reactions positive for the presence of catechol moieties produced a red colour and absorbance was measured at 515 nm. Absorbance values were normalized to OD_{600} of the original culture. Data are presented as the percentage of wild-type extracellular catechol in culture supernatants at 6 h.

Murine virulence assays

DBA/J2 mice (Jackson Laboratories) were infected via intratracheal inoculation as previously described (Heffernan *et al*., 2007). Groups of eight female mice age 6–8 weeks were infected with either wild-type or Δ*fpuB*Δ*fatCD* mutant spores at a dose of 1.5×10^5 spores per mouse. Mice were monitored for 14 days following infection. All mouse experiments were performed using protocols approved by the University of Michigan on the Use and Care of Animals.

Acknowledgements

The authors would like to thank Tyler D. Nusca and David H. Sherman for the kind gift of purified petrobactin. This work was supported in part by a grant (AI169083) from the National Institutes of Health. S.D.D. was supported in part by the American Society for Microbiology (ASM) Robert D. Watkins Graduate Research Fellowship.

References

Abergel, R.J., Wilson, M.K., Arceneaux, J.E., Hoette, T.M., Strong, R.K., Byers, B.R., and Raymond, K.N. (2006a) Anthrax pathogen evades the mammalian immune system through stealth siderophore production. *Proc Natl Acad Sci USA* **103:** 18499–18503.

Abergel, R.J., Wilson, M.K., Arceneaux, J.E.L., Hoette, T.M., Strong, R.K., Byers, B.R., and Raymond, K.N. (2006b) Anthrax pathogen evades the mammalian immune system through stealth siderophore production. *Proc Natl Acad Sci USA* **103:** 18499–18503.

Abergel, R.J., Zawadzka, A.M., and Raymond, K.N. (2008) Petrobactin-mediated iron transport in pathogenic bacteria: coordination chemistry of an unusual 3,4-catecholate/citrate siderophore. *J Am Chem Soc* **130:** 2124–2125.

Almeida, J.L., Harper, B., and Cole, K.D. (2008) *Bacillus anthracis* spore suspensions: determination of stability and comparison of enumeration techniques. *J Appl Microbiol* **104:** 1442–1448.

Arnow, L.E. (1937) Colorimetric determination of the components of 3, 4-dihydroxyphenylalanine–tyrosine mixtures. *J Biol Chem* **118:** 531–537.

Banin, E., Lozinski, A., Brady, K.M., Berenshtein, E., Butterfield, P.W., Moshe, M., *et al*. (2008) The potential of desferrioxamine-gallium as an anti-*Pseudomonas* therapeutic agent. *Proc Natl Acad Sci USA* **105:** 16761–16766.

Barbeau, K., Zhang, G., Live, D.H., and Butler, A. (2002) Petrobactin, a photoreactive siderophore produced by the oil-degrading marine bacterium *Marinobacter hydrocarbonoclasticus*. *J Am Chem Soc* **124:** 378–379.

Beasley, F.C., and Heinrichs, D.E. (2010) Siderophore-mediated iron acquisition in the staphylococci. *J Inorg Biochem* **104:** 282–288.

Braun, V., and Braun, M. (2002) Active transport of iron and siderophore antibiotics. *Curr Opin Microbiol* **5:** 194–201.

Carlson, P.E., Jr, Carr, K.A., Janes, B.K., Anderson, E.C., and Hanna, P.C. (2009) Transcriptional profiling of *Bacillus anthracis* Sterne (34F2) during iron starvation. *PLoS ONE* **4:** e6988.

Carlson, P.E., Jr, Dixon, S.D., Janes, B.K., Carr, K.A., Nusca, T.D., Anderson, E.C., *et al*. (2010) Genetic analysis of petrobactin transport in *Bacillus anthracis*. *Mol Microbiol* **75:** 900–909.

Cendrowski, S., MacArthur, W., and Hanna, P. (2004a) *Bacillus anthracis* requires siderophore biosynthesis for growth in macrophages and mouse virulence. *Mol Microbiol* **51:** 407–417.

Cendrowski, S., MacArthur, W., and Hanna, P. (2004b) *Bacillus anthracis* requires siderophore biosynthesis for growth in macrophages and mouse virulence. *Mol Microbiol* **51:** 407–417.

Challis, G.L. (2005) A widely distributed bacterial pathway for siderophore biosynthesis independent of nonribosomal peptide synthetases. *Chembiochem* **6:** 601–611.

Cowart, R.E. (2002) Reduction of iron by extracellular iron reductases: implications for microbial iron acquisition. *Arch Biochem Biophys* **400:** 273–281.

Davidson, A.L., Dassa, E., Orelle, C., and Chen, J. (2008) Structure, function, and evolution of bacterial ATP-binding cassette systems. *Microbiol Mol Biol Rev* **72:** 317–364, table of contents.

Dixon, T.C., Meselson, M., Guillemin, J., and Hanna, P.C. (1999) Anthrax. *N Engl J Med* **341:** 815–826.

Dixon, T.C., Fadl, A.A., Koehler, T.M., Swanson, J.A., and Hanna, P.C. (2000) Early *Bacillus anthracis*-macrophage interactions: intracellular survival and escape. *Cell Microbiol* **2:** 453–463.

Doganay, L., and Welsby, P.D. (2006) Anthrax: a disease in waiting? *Postgrad Med J* **82:** 754–756.

Dutz, W., and Kohout, E. (1971) Anthrax. *Pathol Annu* **6:** 209–248.

Dutz, W., and Kohout-Dutz, E. (1981) Anthrax. *Int J Dermatol* **20:** 203–206.

Ecker, D.J., and Emery, T. (1983) Iron uptake from ferrichrome A and iron citrate in *Ustilago sphaerogena*. *J Bacteriol* **155:** 616–622.

Eitinger, T., Rodionov, D.A., Grote, M., and Schneider, E. (2011) Canonical and ECF-type ATP-binding cassette importers in prokaryotes: diversity in modular organization and cellular functions. *FEMS Microbiol Rev* **35:** 3–67.

Faraldo-Gomez, J.D., and Sansom, M.S. (2003) Acquisition of siderophores in gram-negative bacteria. *Nat Rev Mol Cell Biol* **4:** 105–116.

Fox, D.T., Hotta, K., Kim, C.Y., and Koppisch, A.T. (2008) The missing link in petrobactin biosynthesis: asbF encodes a (–)-3-dehydroshikimate dehydratase. *Biochemistry* **47:** 12251–12253.

Garénaux, A., Caza, M., and Dozois, C.M. (2011) The Ins and Outs of siderophore mediated iron uptake by extraintestinal pathogenic *Escherichia coli*. *Vet Microbiol* **153:** 89–98.

Garner, B.L., Arceneaux, J.E., and Byers, B.R. (2004) Temperature control of a 3,4-dihydroxybenzoate (protocatechuate)-based siderophore in *Bacillus anthracis*. *Curr Microbiol* **49:** 89–94.

Glanfield, A., McManus, D.P., Anderson, G.J., and Jones, M.K. (2007) Pumping iron: a potential target for novel therapeutics against schistosomes. *Trends Parasitol* **23:** 583–588.

Guidi-Rontani, C., Weber-Levy, M., Labruyere, E., and Mock, M. (1999) Germination of *Bacillus anthracis* spores within alveolar macrophages. *Mol Microbiol* **31:** 9–17.

Hanna, P. (1998a) Anthrax pathogenesis and host response. *Curr Top Microbiol Immunol* **225:** 13–35.

Hanna, P. (1998b) How anthrax kills. *Science* **280:** 1673–1674.

Heffernan, B.J., Thomason, B., Herring-Palmer, A., and Hanna, P. (2007) *Bacillus anthracis* anthrolysin O and three phospholipases C are functionally redundant in a murine model of inhalation anthrax. *FEMS Microbiol Lett* **271:** 98–105.

Hotta, K., Kim, C.Y., Fox, D.T., and Koppisch, A.T. (2010) Siderophore-mediated iron acquisition in *Bacillus anthracis* and related strains. *Microbiology* **156:** 1918–1925.

Inglesby, T.V., Henderson, D.A., Bartlett, J.G., Ascher, M.S., Eitzen, E., Friedlander, A.M., *et al.* (1999) Anthrax as a biological weapon: medical and public health management. Working group on civilian biodefense. *JAMA* **281:** 1735–1745.

Inglesby, T.V., O'Toole, T., Henderson, D.A., Bartlett, J.G., Ascher, M.S., Eitzen, E., *et al.* (2002) Anthrax as a biological weapon, 2002: updated recommendations for management. *JAMA* **287:** 2236–2252.

Janes, B.K., and Stibitz, S. (2006) Routine markerless gene replacement in *Bacillus anthracis*. *Infect Immun* **74:** 1949–1953.

Kadi, N., and Challis, G.L. (2009) Chapter 17. Siderophore biosynthesis a substrate specificity assay for nonribosomal peptide synthetase-independent siderophore synthetases involving trapping of acyl-adenylate intermediates with hydroxylamine. *Methods Enzymol* **458:** 431–457.

Koppisch, A.T., Browder, C.C., Moe, A.L., Shelley, J.T., Kinkel, B.A., Hersman, L.E., *et al.* (2005) Petrobactin is the primary siderophore synthesized by *Bacillus anthracis* str. Sterne under conditions of iron starvation. *Biometals* **18:** 577–585.

Koppisch, A., Dhungana, S., Hill, K., Boukhalfa, H., Heine, H., Colip, L., *et al.* (2008a) Petrobactin is produced by both pathogenic and non-pathogenic isolates of the *Bacillus cereus* group of bacteria. *Biometals* **21:** 581–589.

Koppisch, A.T., Hotta, K., Fox, D.T., Ruggiero, C.E., Kim, C.Y., Sanchez, T., *et al.* (2008b) Biosynthesis of the 3,4-dihydroxybenzoate moieties of petrobactin by *Bacillus anthracis*. *J Org Chem* **73:** 5759–5765.

Koster, W. (2001) ABC transporter-mediated uptake of iron, siderophores, heme and vitamin B12. *Res Microbiol* **152:** 291–301.

Koster, W. (2005) Cytoplasmic membrane iron permease systems in the bacterial cell envelope. *Front Biosci* **10:** 462–477.

Koster, W., and Braun, V. (1990a) Iron (III) hydroxamate transport into *Escherichia coli*. Substrate binding to the periplasmic FhuD protein. *J Biol Chem* **265:** 21407–21410.

Koster, W., and Braun, V. (1990b) Iron(III) hydroxamate transport of *Escherichia coli*: restoration of iron supply by coexpression of the N- and C-terminal halves of the cytoplasmic membrane protein FhuB cloned on separate plasmids. *Mol Gen Genet* **223:** 379–384.

Koster, W.L., Actis, L.A., Waldbeser, L.S., Tolmasky, M.E., and Crosa, J.H. (1991) Molecular characterization of the iron transport system mediated by the pJM1 plasmid in *Vibrio anguillarum* 775. *J Biol Chem* **266:** 23829–23833.

Lee, J.Y., Janes, B.K., Passalacqua, K.D., Pfleger, B.F., Bergman, N.H., Liu, H., *et al.* (2007) Biosynthetic analysis

of the petrobactin siderophore pathway from *Bacillus anthracis*. *J Bacteriol* **189:** 1698–1710.
Lee, J.Y., Passalacqua, K.D., Hanna, P.C., and Sherman, D.H. (2011) Regulation of petrobactin and bacillibactin biosynthesis in *Bacillus anthracis* under iron and oxygen variation. *PLoS ONE* **6:** e20777.
Liu, H., Hakansson, K., Lee, J.Y., and Sherman, D.H. (2007) Collision-activated dissociation, infrared multiphoton dissociation, and electron capture dissociation of the *Bacillus anthracis* siderophore petrobactin and its metal ion complexes. *J Am Soc Mass Spectrom* **18:** 842–849.
Lopez, C.S., and Crosa, J.H. (2007) Characterization of ferric-anguibactin transport in *Vibrio anguillarum*. *Biometals* **20:** 393–403.
Marion, C., Aten, A.E., Woodiga, S.A., and King, S.J. (2011) Identification of an ATPase, MsmK, which energizes multiple carbohydrate ABC transporters in *Streptococcus pneumoniae*. *Infect Immun* **79:** 4193–4200.
Miethke, M., and Marahiel, M.A. (2007) Siderophore-based iron acquisition and pathogen control. *Microbiol Mol Biol Rev* **71:** 413–451.
Miethke, M., Klotz, O., Linne, U., May, J.J., Beckering, C.L., and Marahiel, M.A. (2006) Ferri-bacillibactin uptake and hydrolysis in *Bacillus subtilis*. *Mol Microbiol* **61:** 1413–1427.
Neilands, J.B. (1995) Siderophores: structure and function of microbial iron transport compounds. *J Biol Chem* **270:** 26723–26726.
Nicholson, W.L., Munakata, N., Horneck, G., Melosh, H.J., and Setlow, P. (2000) Resistance of *Bacillus* endospores to extreme terrestrial and extraterrestrial environments. *Microbiol Mol Biol Rev* **64:** 548–572.
Olakanmi, O., Britigan, B.E., and Schlesinger, L.S. (2000) Gallium disrupts iron metabolism of mycobacteria residing within human macrophages. *Infect Immun* **68:** 5619–5627.
Oves-Costales, D., Kadi, N., Fogg, M.J., Song, L., Wilson, K.S., and Challis, G.L. (2007) Enzymatic logic of anthrax stealth siderophore biosynthesis: AsbA catalyzes ATP-dependent condensation of citric acid and spermidine. *J Am Chem Soc* **129:** 8416–8417.
Oves-Costales, D., Kadi, N., Fogg, M.J., Song, L., Wilson, K.S., and Challis, G.L. (2008) Petrobactin biosynthesis: AsbB catalyzes condensation of spermidine with N(8)-citryl-spermidine and its N(1)-(3,4-dihydroxybenzoyl) derivative. *Chem Commun (Camb)* **34:** 4034–4036.
Oves-Costales, D., Kadi, N., and Challis, G.L. (2009) The long-overlooked enzymology of a nonribosomal peptide synthetase-independent pathway for virulence-conferring siderophore biosynthesis. *Chem Commun* **43:** 6530–6541.
Passalacqua, K.D., and Bergman, N.H. (2006) *Bacillus anthracis*: interactions with the host and establishment of inhalational anthrax. *Future Microbiol* **1:** 397–415.
Pfleger, B.F., Lee, J.Y., Somu, R.V., Aldrich, C.C., Hanna, P.C., and Sherman, D.H. (2007) Characterization and analysis of early enzymes for petrobactin biosynthesis in *Bacillus anthracis*. *Biochemistry* **46:** 4147–4157.
Pfleger, B.F., Kim, Y., Nusca, T.D., Maltseva, N., Lee, J.Y., Rath, C.M., *et al*. (2008a) Structural and functional analysis of AsbF: origin of the stealth 3,4-dihydroxybenzoic acid subunit for petrobactin biosynthesis. *Proc Natl Acad Sci USA* **105:** 17133–17138.
Pfleger, B.F., Kim, Y., Nusca, T.D., Maltseva, N., Lee, J.Y., Rath, C.M., *et al*. (2008b) Structural and functional analysis of AsbF: origin of the stealth 3,4-dihydroxybenzoic acid subunit for petrobactin biosynthesis. *Proc Natl Acad Sci USA* **105:** 17133–17138.
Ratledge, C. (2004) Iron, mycobacteria and tuberculosis. *Tuberculosis (Edinb)* **84:** 110–130.
Ratledge, C., and Dover, L.G. (2000) Iron metabolism in pathogenic bacteria. *Annu Rev Microbiol* **54:** 881–941.
Spencer, R.C. (2003) *Bacillus anthracis*. *J Clin Pathol* **56:** 182–187.
Sterne, M. (1939) The immunization of laboratory animals against anthrax. *Onderstepoort J Vet Sci Anim Ind* **13:** 313–317.
Sweeney, D.A., Hicks, C.W., Cui, X., Li, Y., and Eichacker, P.Q. (2011) Anthrax infection. *Am J Respir Crit Care Med* **184:** 1333–1341.
Wandersman, C., and Delepelaire, P. (2004) Bacterial iron sources: from siderophores to hemophores. *Annu Rev Microbiol* **58:** 611–647.
Wilson, M.K., Abergel, R.J., Raymond, K.N., Arceneaux, J.E., and Byers, B.R. (2006) Siderophores of *Bacillus anthracis, Bacillus cereus*, and *Bacillus thuringiensis*. *Biochem Biophys Res Commun* **348:** 320–325.
Wilson, M.K., Abergel, R.J., Arceneaux, J.E., Raymond, K.N., and Byers, B.R. (2009) Temporal production of the two *Bacillus anthracis* siderophores, petrobactin and bacillibactin. *Biometals* **23:** 129–134.
Wilson, M.J., Carlson, P.E., Janes, B.K., and Hanna, P.C. (2012) Membrane topology of the *Bacillus anthracis* GerH germinant receptor proteins. *J Bacteriol* **194:** 1369–1377.
Wooldridge, K.G., Morrissey, J.A., and Williams, P.H. (1992) Transport of ferric-aerobactin into the periplasm and cytoplasm of *Escherichia coli* K12: role of envelope-associated proteins and effect of endogenous siderophores. *J Gen Microbiol* **138:** 597–603.
Zawadzka, A.M., Abergel, R.J., Nichiporuk, R., Andersen, U.N., and Raymond, K.N. (2009a) Siderophore-mediated iron acquisition systems in *Bacillus cereus*: identification of receptors for anthrax virulence-associated petrobactin. *Biochemistry* **48:** 3645–3657.
Zawadzka, A.M., Kim, Y., Maltseva, N., Nichiporuk, R., Fan, Y., Joachimiak, A., and Raymond, K.N. (2009b) Characterization of a *Bacillus subtilis* transporter for petrobactin, an anthrax stealth siderophore. *Proc Natl Acad Sci USA* **106:** 21854–21859.

Supporting information

Additional supporting information may be found in the online version of this article.

Please note: Wiley-Blackwell are not responsible for the content or functionality of any supporting materials supplied by the authors. Any queries (other than missing material) should be directed to the corresponding author for the article.